

Learning for Interval Prediction of Electricity Demand: A Cluster-based Bootstrapping Approach

Rohit Dube^a, Natarajan Gautam^b, Amarnath Banerjee^a, Harsha
Nagarajan^c

^a*Industrial and Systems Engineering, Texas A & M University,
College Station, 77843, TX, USA*

^b*Electrical Engineering and Computer Science, Syracuse University,
Syracuse, 13210, NY, USA*

^c*Applied Mathematics and Plasma Physics, Los Alamos National Laboratory,
Los Alamos, 87545, NM, USA*

Abstract

Accurate predictions of electricity demands are necessary for managing operations in a small aggregation load setting like a Microgrid. Due to low aggregation, the electricity demands can be highly stochastic and point estimates would lead to inflated errors. Interval estimation in this scenario, would provide a range of values within which the future values might lie and helps quantify the errors around the point estimates. This paper introduces a residual bootstrap algorithm to generate interval estimates of day-ahead electricity demand. A machine learning algorithm is used to obtain the point estimates of electricity demand and respective residuals on the training set. The obtained residuals are stored in memory and the memory is further partitioned. Days with similar demand patterns are grouped in clusters using an unsupervised learning algorithm and these clusters are used to partition the memory. The point estimates for test day are used to find the closest cluster of similar days and the residuals are bootstrapped from the chosen cluster. This algorithm is evaluated on the real electricity demand data from EULR (End Use Load Research) and is compared to other bootstrapping methods for varying confidence intervals.

Keywords: Time Series, Load Forecasting, Confidence Intervals, Machine Learning, Residual Errors.

Nomenclature

Notations

J	Set of training days, viz. $J=\{1, 2, \dots, 365\}$
j	Index of the days in training set $j \in J$
J'	Set of test days, viz. $J'=\{1, 2, \dots, 90\}$
j'	Index of the days in test set $j' \in J'$
I	Set of 15-minute time interval in a day, viz. $I=\{1, 2, \dots, 96\}$
i	Index of the 15-minute time interval in a day $i \in I$
\mathbf{X}_i^j	Vector of input variables for ML model at time i and day j
y_i^j (\hat{y}_i^j)	Observed (predicted) electricity demand at the time i and day j
y^j	Vector of observed demand for the j_{th} day $y^j = (y_1^j, y_2^j, y_3^j, \dots, y_{96}^j)$
z_i^j	Observed residual error of the ML model $z_i^j = y_i^j - \hat{y}_i^j$
z^j	Vector of residual errors for the j_{th} day $z^j = (z_1^j, z_2^j, z_3^j, \dots, z_{96}^j)$
$\hat{z}_i^{j'}$	Estimate of residual error $z_i^{j'}$
$ I , J , J' $	Cardinality of set I , J , and J' respectively
E	Memory set of training residuals $E = \{z^1, \dots, z^{365}\}$
N	Number of bootstrap replicates

Abbreviations

ACF	Auto-Correlation Function
ANN	Artificial Neural Networks
CBB	Cluster-based Block Bootstrapping
EULR	End Use Load Research
GBR	Gradient Boosting Regression

ISO	Independent System Operators
LGBM	Light Gradient Boosting Machine
LR	Linear Regression
MAE	Mean Absolute Error
MAPE	Mean Absolute Percentage Error
ML	Machine Learning
MSE	Mean Squared Error
PACF	Partial Auto-Correlation Function
R ²	R Squared Error
RMSE	Root Mean Squared Error
RMSLE	Root Mean Squared Logarithm Error
<i>WSS</i>	Within-cluster Sum of Squares

1. Introduction

The past few decades have led to the emergence of deregulated electricity markets resulting in Independent System Operators (ISO) allowing participants to buy and sell electricity in the market. The ISOs, such as the New England ISO and Electric Reliability Council of Texas (ERCOT), conduct market settlement of prices for electricity for supply and demand mainly at two-time levels called day-ahead followed by real-time markets. Consumers of electricity such as local residential microgrids defined as a group of interconnected loads with distributed energy generation, are envisioned to participate in the day-ahead markets to avoid the volatility of electricity prices in real-time markets. In order to do so, the microgrids require accurate day-ahead forecasts of electricity demands for the next 24-32 hours. However, there are difficulties associated with multi-horizon load forecasting, especially in residential microgrids due to lower load aggregation. The effect of low aggregation is represented in Figure 1 where the average electricity demand of 10 houses is compared with the 150 houses.

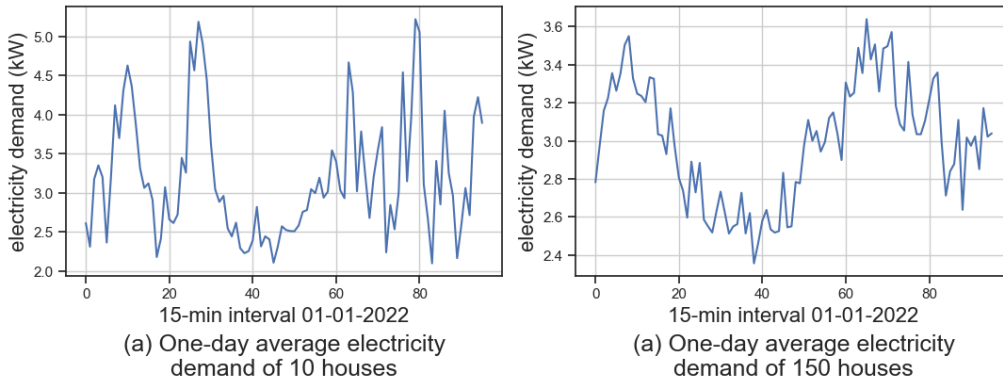


Figure 1: Stochasticity of electricity demand in the EULR dataset [Northwest Energy Efficiency Alliance \(2020\)](#) due to varying levels of aggregation.

Additionally, the pattern of electricity demand in the residential sector is non-stationary and periodic over daily, weekly, and annual cycles which makes the forecasting of electricity demand a difficult problem. This, along with locally distributed energy generation from solar photovoltaic and wind turbines, low aggregation of consumption units, and newer loads like Electric Vehicles leads to high volatility as the random noise from these sources is superimposed on the daily demand curve. The microgrids, however, offer advantages such as improved reliability and resiliency by providing backup during grid outages, increased renewable energy use, cost savings, and consumer-side control. Accurate prediction of energy demand and generation is necessary to reduce demand costs and meet the energy demands in microgrids.

The forecasting requirements of microgrids can broadly range from days, hours, or real-time (short-term) for optimizing energy generation and distribution to several months (long-term) for scheduling maintenance, capacity planning, and policy formulation. Short-term prediction of one-day-ahead demand is defined as the process of forecasting the expected electricity demand of the microgrid over a short time horizon, in the case of this research, the next day. Short-term point forecasts of electricity demands have been traditionally used and extensively researched ([Fildes et al. \(1997\)](#), [Lago et al. \(2021\)](#)) and are an essential tool to plan generation schedules for electricity in the day-ahead energy markets. The application of short-term forecasting thus is to identify the demand cycle, accounting for the random noise while considering consistent noise deviations for the following day.

Traditionally, point forecasting the expected electricity demand has dom-

inated literature (Harvey et al. (1993); Espinoza et al. (2005); Clements et al. (2016); Hippert et al. (2001)). But in the case of microgrids, electricity demand is extremely volatile, much due to the renewable energy generation and low aggregation of demand loads. The point estimates cannot represent the entire information accurately as a result of the noise and stochastic nature of demands. Thus forecasting prediction intervals are preferred over point forecasts as they provide the range of possible outcomes for demand (Li et al. (2017)) rather than predicting the volatile demand. The estimate of prediction intervals along with point forecasts becomes an important tool for cost-saving policies and decision-making for power system operations (Hong and Fan (2016)) as decisions can be made for many future scenarios. In the context of robust optimization, accurate demand interval predictions can be useful to form uncertainty sets. Robust reconfiguration of microgrids with an accurate prediction of intervals can lead to better solution strategies (Lee et al. (2015)).

Machine Learning (ML) models have been growing in popularity for forecasting point and interval prediction of electric load (Mori and Kobayashi (1996); Ahmad et al. (2014); Kong et al. (2019); Zhang et al. (2013); Mocanu et al. (2016)) with a major emphasis on Linear Regression (LR) and Artificial Neural Networks (ANN). We will use the residuals obtained by ML models to form prediction intervals by bootstrapping residuals, but before doing so we will consider the problem associated with direct bootstrapping. An important assumption in ML models is that the model errors are independent and identically distributed (IID) implying that the residuals have no trends and are not connected to each other in any way. Bootstrap re-sampling developed by Efron (1979) is a procedure to generate a sampling distribution by repeatedly taking random samples from the known sample, with replacement. The methods available for bootstrapping depend on whether the input data for the method is an independent random variable or a time series (Hrdle et al. (2003)). As seen later in the section 4 there is an auto-correlation present in the residual series of electricity demand, block bootstrap is used instead of the normal bootstrap. Instead of single sample points, contiguous sections of time series are selected at random and joined together, maintaining the structural dependence or auto-correlations of the residuals required by time-series bootstrap methods. A similar approach is shown in Bergmeir et al. (2016) where the moving block bootstrap developed by Mignani and Rosa (1995) is used to sample from the residual series. LOESS (Locally Estimated Scatterplot Smoothing) developed by Cleveland et al. (1990) is used to obtain the

residuals by applying seasonal-trend decomposition to the observations.

Recently, tree-based ensemble models were one of the top performers in the M5 and Global Energy Forecasting (GEFCom) competition and are one of the leading models used on Kaggle (Bojer and Meldgaard (2021)). The performance of ensemble models on time-series data in the mentioned competitions is a major drive to test these models for forecasting in this research. While the recent results of ensemble models show potential, forecasting based on Linear Regression and Artificial Neural Networks have been used vastly. We train the tree ensemble point forecast models of Light Gradient Boosting Machine (LGBM) and Gradient Boosting Regression (GBR) as well as Linear Regression (LR) with exogenous variables.

Assuming that the future residuals of time series will be like the past, i.e, stationary residuals, the future residual errors can be sampled multiple times from the ones seen in the past to simulate an entire set of future values for time series (Stine (1985), Clements and Kim (2007), Pan and Politis (2016)). However, we shall see that the residuals of the electricity demand obtained by ML models are non-stationary, as the ML model has a higher residual error during the months of high electricity demand and is lower residual values otherwise. We observe that the residuals of days with similar electricity demand patterns are similar, thus the paper proposes a cluster-based method to tackle the problem of non-stationarity. The proposed procedure is to cluster the residuals of the day with similar demand patterns together. The residual errors of the days within each cluster in the memory appear to have a near-constant variance. A similarity score can be assigned to the point estimates of the day-ahead demand and all the clusters and the residuals can be bootstrapped from the cluster with the best similarity score. The proposed method, called cluster-based block bootstrap, solves the two problems associated with non-IID structure and non-stationarity with block bootstrapping and clustering respectively.

With that motivation, the objective of this paper is two-fold; first is to develop a non-parametric bootstrap algorithm to generate prediction intervals of day-ahead electricity demand with high confidence based on a point estimate ML model, and second is to reduce the computation time required by the proposed algorithm compared to the bootstrap aggregating models.

The paper proceeds with the introduction of the electricity demand data in Section 2, problem definition, and the results of point estimates are described in Section 3 and Section 4. We propose the Cluster Block Bootstrap algorithm in Section 5. The results of the proposed algorithms are com-

pared to other bootstrapping algorithms in Section 6. We show that the proposed algorithm achieves the performance of the baseline algorithm with a considerable decrease in computation time.

2. Data

ML models have the limitation of needing large amounts of data for accurate prediction. Large-scale electric load data collection projects like residential End Use Load Research (EULR) by Northwest Energy Efficiency Alliance ([Northwest Energy Efficiency Alliance \(2020\)](#)) and Pecan Street Austin ([Pecan Street Inc. Dataport](#)) have provided the spatial and temporal granularity to work with the ML models requiring vast amounts of training data. EULR data on electricity demand was collected at 1-minute intervals from 400 homes across the Northwestern region of the states of Washington, Oregon, Montana, and Idaho. The information about temperature, humidity, and other atmospheric conditions is provided in the EULR data.

It is worthwhile to describe the EULR project before we go into the details of the model. The EULR project is a regional study designed to gather accurate electricity demand profiles that could help us in understanding contemporary electricity end-use patterns. While the project collects data for every minute interval, it has provided public access to the 15-minute interval data of electricity demand in residential and commercial units for research purposes. Each of the units is called sites, with each site recognized by its *unique id*. Since the inception of the project in 2020, data has been collected from around 400 such sites, including solar-powered sites.

The data provided in EULR consists of electricity drawn by the residential site’s main supply line as well as at some of the major electrical appliances. The sites with solar generation are labeled as such and can be filtered out from the dataset. For such sites, data on net electricity consumed by the main supply line is provided. Thus the time series of electricity demand and solar generation cannot be separated for sites with solar generation. As a result, in this paper, we train our models on the electricity demand registered at the site’s main supply line without any solar power generation. Compared to all the states mentioned earlier, the data for the highest number of residential sites were recorded in Washington state. The number of units from Washington for which data were continuously collected from the year 2020 to 2022 is 50. This is still considerably low and thus creates a scenario where prediction for fewer households is needed as in a small Microgrid.

Figure 2 shows the one-day moving average (96 intervals of 15 minutes) for the aggregate electricity demand of these 50 sites. The effects of annual seasonality can be seen as there is a downward trend in demand from the month of March to May and an upward trend from October to January. We describe the ML models in Section 3 for which data from the year 2021 is used as a training sample and the data from the first quarter of 2022 is used for testing. The train-test split will remain the same in all of the following sections. We begin defining the problem setup and show the results of ML point estimates in the following section.

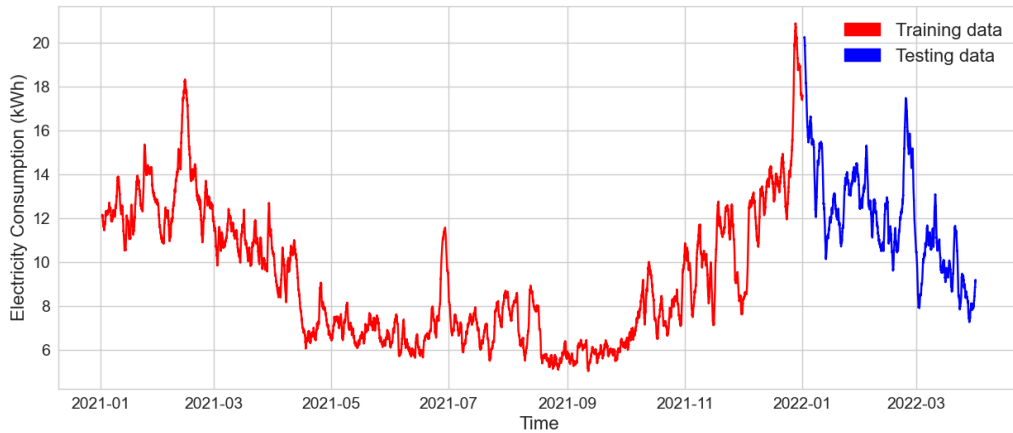


Figure 2: One-day moving average of aggregate electricity demand for 50 sites in Washington

3. Problem Definition

The objective of this study is to accurately forecast the prediction interval of the one-day-ahead aggregate electricity demand of the 50 residential sites. The interval prediction model in this research is based on residuals obtained from point estimates of the ML model’s forecast. This section explains the inputs to the ML model and compares the results of the point estimates of the implemented ML models. Furthermore, Section 4 formalizes the results of the point estimates discussed here and presents the necessary elements required for interval prediction.

Recall from Section 2 that the data from the year 2021 is used as the training data. Each day in the training set is represented by j where $j \in$

$J = \{1, 2, \dots, 365\}$. Further, the daily aggregated demand can be divided into 96 intervals represented by i such that $i \in I = \{1, 2 \dots, 96\}$ with $i = 1$ representing time 00 : 00 : 00, sequentially increasing in intervals of 15 minutes until 23 : 45 : 00. The training data for time series can be considered as labeled data of the form (\mathbf{X}_i^j, y_i^j) , where \mathbf{X}_i^j is the input vector comprising of the lags and exogenous variables and y_i^j is the observed demand for the i_{th} interval on a j_{th} day. The input lag and exogenous variables for the ML model are selected as follows.

3.1. Input Variable Selection

The plot of the Partial Auto-Correlation Function (PACF) is used by auto-regressive models to measure the correlation between the observed values of time-series (Elsaraiti et al. (2021)), in our case, the electricity demand of y_i^j to y_{i-k}^j for different values of k . The PACF for electricity demand data on the training set is plotted on the right-hand side of Figure 3 which shows the dependence of the demand y_i^j on y_{i-1}^j and y_{i-2}^j values. It should be noted that since we are making a multi-horizon prediction for a one-day ahead period, the lag values or the observed data during the $i - 1$ and $i - 2$, for $i > 1$ wouldn't be available for i_{th} interval prediction. However, the Auto-correlation function (ACF) in the left-hand side of Figure 3 suggests that the electricity demand during the interval i is correlated with the demand seen during the same interval of the previous day. Thus, using these observations from the PACF and ACF plots, observed values of y_{i-1}^{j-1} and y_{i-2}^{j-1} can serve as a naive estimate for the two lag input variables for the prediction of demand in interval i .

We shall now look at the input exogenous variables used by the ML model. The calendar effects of a quarterly period of a year and holidays including weekends and national holidays are shown to affect electricity demand (Son et al. (2022), U.S. Energy Information Administration). Also, the dependence of the electricity demand on temperature is seen in Figure 4 where more electricity is required at lower temperatures indicating the use of space heating units and at higher temperatures as a result of using space cooling units in residential sites. The temperature for any interval for a given day is the day-ahead predicted temperature from the nearest NOAA (National Oceanic and Atmospheric Administration) station. Thus, quarterly effects, holidays, and temperature predictions are considered as the input exogenous variables to the ML model.

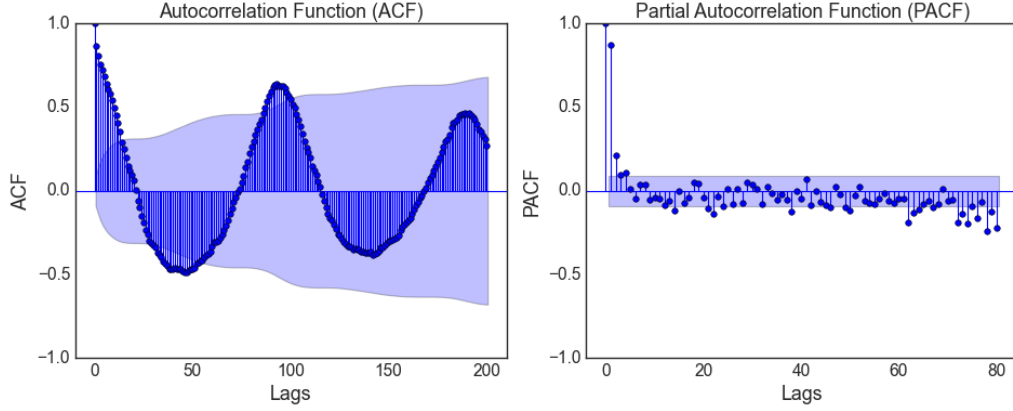


Figure 3: ACF plot (left) and PACF plot (right) of electricity demand

Considering lag and exogenous variables, the input vector \mathbf{X}_i^j for j th day and i th interval is thus defined as follows.

$$\mathbf{X}_i^j = (x_{i1}^j, x_{i2}^j, x_{i3}^j, x_{i4}^j, x_{i5}^j)$$

where,

$$\begin{aligned} x_{i1}^j &= y_{i-1}^{j-1} && \text{naive estimate for input lag variable of } y_{i-1}^j, \\ x_{i2}^j &= y_{i-2}^{j-1} && \text{naive estimate for input lag variable of } y_{i-2}^j, \\ x_{i3}^j &= \text{predicted temperature in Fahrenheit,} \\ x_{i4}^j &= \begin{cases} 0 & \text{Jan-Mar} \\ 1 & \text{Apr-Jun} \\ 2 & \text{Jul-Sep} \\ 3 & \text{Oct-Dec,} \end{cases} \\ x_{i5}^j &= \begin{cases} 1 & \text{Holidays and Weekends (Saturday and Sunday)} \\ 0 & \text{other days.} \end{cases} \end{aligned}$$

We consider the ML model of the form $\hat{y}_i^t = \hat{f}(\mathbf{X}_i^j)$, where \hat{f} is a real-valued function approximated by ML models. The usual assumption on the residual errors of such a model here denoted by $z_i^j = y_i^j - \hat{y}_i^j$ is that they are IID. As can be seen in Figure 5, the residuals are centered around 0 and the variance of the residuals is higher in the months of January to March, decreases until July, and again increases from August to December.

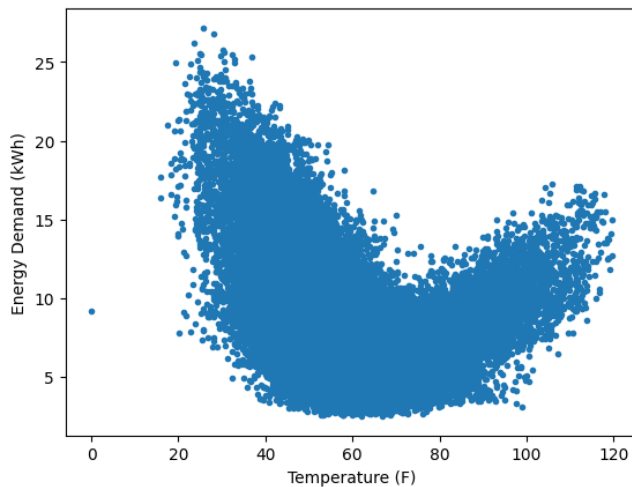


Figure 4: Temperature vs Electricity Demand

This residual pattern follows the electricity demand with higher variance during the days of higher electricity demand and vice versa, representing non-stationarity.

3.2. Point Estimate Metrics

The point estimates on the testing set are generated by an expanding window technique on the training set. The current test day observations are added to the training set and a new training model is obtained for the next test day predictions. The moving window proceeds by first predicting the day ahead demand and then adding the labeled data $\mathbf{X}_i^{j'}$ of the day j' to the training set, where $j' \in J' = \{1, 2, \dots, 90\}$ denotes the label of test days.

The model errors of the training and testing data are shown in Table 1. The absolute deviations from the observed demand are highest for GBR on test data compared to LR and LGBM. The lower error metrics on the LGBM model denote better point estimates on the test set.

ML models are susceptible to over-fitting on the training set resulting in the lower error on the training set and higher errors on the test set. If the training errors are directly bootstrapped for the interval estimation of the test day, the intervals would be narrow due to the over-fitting problem. We overcome this problem by replacing the errors of the training set with the errors on the test set sequentially, which is further described in Section 5.

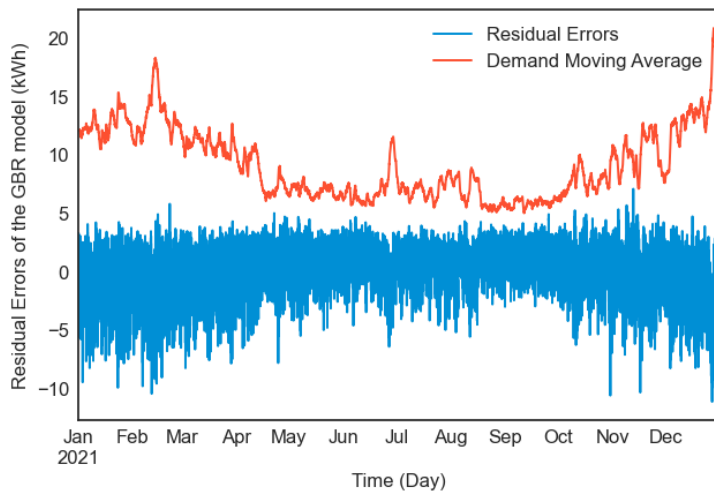


Figure 5: Residual errors of GBR on the training set with moving average of observed demand

4. Interval Estimation

The proposed model of the construction of prediction intervals or interval estimation of the electricity demand involves the use of residual errors obtained by the ML models seen in the previous section. We define and formalize the need for residual blocks and the memory clusters in this section that will be used for bootstrapping.

Scores	LR		GBR		LGBM	
	Train	Test	Train	Test	Train	Test
MAE	1.3458	1.6712	1.6169	1.7674	1.2116	1.5947
MSE	3.0945	4.5004	4.1095	5.1656	2.5399	4.0726
RSME	1.7591	2.1214	2.0272	2.2728	1.5937	2.0181
MAPE	15.27%	14.39%	18.05%	15.71%	13.69%	13.64%
R2	0.7452	0.5301	0.3334	0.5231	0.7976	0.5521
RMSLE	0.1709	0.1662	0.2114	0.1736	0.1541	0.1602

Table 1: Model performance for point forecasts

4.1. Residual Block

There are several methods to obtain the prediction intervals so that the future value of electricity demand could lie within the interval with a relatively high probability. We adopt a non-parametric approach where the residual errors are re-sampled in order to build the prediction intervals. We begin by building up notation for the residual errors. The observed forecast error on the training data for the ML model is given as follows

$$z_i^j = y_i^j - \hat{y}_i^j \quad \forall i \in I, j \in J \quad (1)$$

where y_i^j is the observed demand and \hat{y}_i^j is the predicted demand by the ML models. We define a memory set E such that the elements are a tuple of the j th day errors, thus for the training set we can define E as

$$E = \{(z_1^1, z_2^1, \dots, z_{96}^1), \dots, (z_1^j, z_2^j, \dots, z_{96}^j), \dots, (z_1^{365}, z_2^{365}, \dots, z_{96}^{365})\}. \quad (2)$$

Then the residual errors for test data are given by

$$\begin{aligned} z_i^{j'} &= y_i^{j'} - \hat{y}_i^{j'} \quad \forall i \in I, j' \in J' \\ y_i^{j'} &= \hat{y}_i^{j'} + z_i^{j'}. \end{aligned} \quad (3)$$

The prediction interval for $y_i^{j'}$ can be built by bootstrapping for $z_i^{j'}$ from the residual error set E , such that $y_i^{j'} = \hat{y}_i^{j'} + \hat{z}_i^{j'}$ if the errors are identically distributed. Thus, we shall first discuss the case of the traditional IID bootstrap method. This method considers that the future errors of the test set are similar to the past errors so that $\hat{z}_i^{j'}$ can be approximated with the bootstrapped values of the residual errors from the training set z_i^j . Thus the residuals could be randomly selected with replacement from the memory set of the training residual errors E , N times, where N is some large valued integer. Suppose $N = 1000$, and $(z_{(1)}^*, z_{(2)}^*, \dots, z_{(1000)}^*)_{i}^{j'}$ is the ordered set of the bootstrapped residuals for day j' and interval i randomly selected from memory E with replacement, then the 5th and the 95th percentile values of the prediction interval are represented by $z_{(5)}^*$ and $z_{(950)}^*$, respectively.

However, the ACF and PACF plots of the residual series \hat{z}_i^j presented in Figure 6 indicate the existence of correlation among the residuals. As a result of this, the IID bootstrap cannot be applied to the dependent data of residual electricity demand. Also, there are variations in the magnitude of the residuals on the training set as seen in Figure 5 indicating that the errors

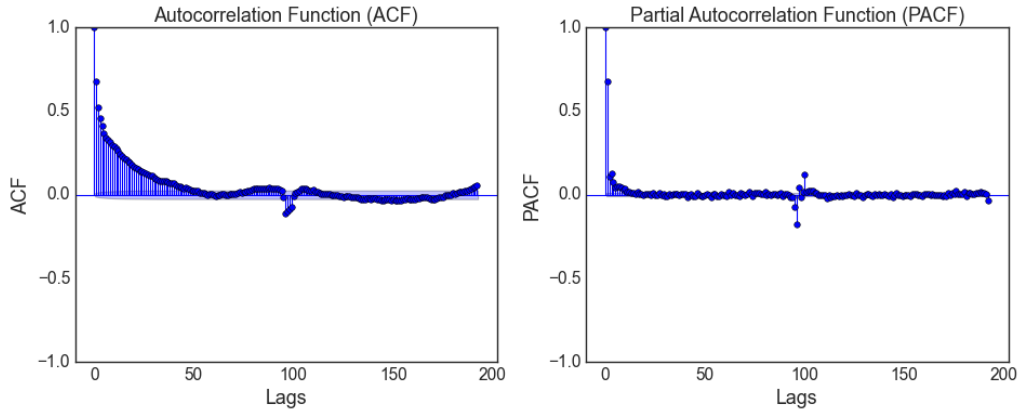


Figure 6: ACF plot (left) and PACF plot (right) of residuals of ML model

are not identical. The inadequacy of the IID bootstrap method for dependent series is described in [Singh \(1981\)](#). Instead of re-sampling a single observation of residuals at a time, non-overlapping contiguous blocks of residuals can be re-sampled. As a result, the structural dependence of the residuals can be preserved. Thus the residual of the electricity demand isn't randomly selected from the memory E and in order to account for the correlations among the errors, non-overlapping blocks of fixed length are drawn from the observed residual set and then joined. A day is divided into 96 intervals of 15 minutes, where $n = 96$ which can be split into b consecutive blocks of equal length l . We define the residual vector and the splitting rule as follows

$$z^j = (z_1^j, z_2^j, z_3^j, \dots, z_n^j) \quad \forall j \in J, \quad (4)$$

$$z^j = (B_1^j, \dots, B_b^j), \quad (5)$$

$$\text{such that } B_k = (z_{(k-1)l+1}, \dots, z_{kl}), \quad k = (1, \dots, b),$$

where the residual errors on the training data for j_{th} day are given as a vector z^j , and the elements of this vector are calculated using Equation (1).

The accuracy of the block bootstrap is sensitive to the size of the blocks. As suggested in [Politis and White \(2006\)](#), the empirical block length of $n^{1/3}$ would be a good guess for the block length l .

4.2. Clustering

The demand levels affect residual errors in a way where the errors are higher for higher levels of demand patterns and low for lower demands. Thus,

instead of random block bootstrapping from the set E on j 'th day, we bootstrap from a cluster of similar days. The idea here is to group together the days from the training set with similar demand levels in a cluster and then block bootstrap from the cluster representative of the test day. Such clusters can be created by measuring the similarity between different days and can be achieved by various unsupervised learning methods. A common unsupervised learning algorithm for creating labeled clusters is called k-means clustering (Hartigan and Wong (1979)).

Then the k-means clustering algorithm takes the number of clusters (N_c) and the set of observed vectors to clusters. It then returns a set of centroids, one for each of the N_c clusters where the observation vector is classified with the cluster number (C_i) or centroid index of the centroid closest to it. The k-means clustering algorithm tries to minimize the within-cluster sum-of-squares (WSS) between each observation vector and its dominating centroid. The minimization is achieved by iterative reclassification of the set of vectors into new clusters and recalculating the centroids. Since there is no prior knowledge about the value of N_c , we will heuristically choose N_c by using the elbow method as shown in Figure 7. Suppose the day's demand with n intervals of the electricity demand for the j th day is represented by the vector y^j , such that:

$$y^j = (y_1^j, y_2^j, y_3^j, \dots, y_n^j) \quad \forall j \in J \quad (6)$$

then the WSS (WSS) is given as follows:

$$WSS = \sum_{k=1}^{N_c} \sum_{y^j \in C_k} d(y^j, \bar{y}_{C_k}) \quad (7)$$

where,

- N_c = number of clusters,
- C_k = index of a cluster,
- $d(\cdot)$ = distance metric between two vectors,
- \bar{y}_{C_k} = center of the centroid C_k .

The k-means clustering algorithm can be run for multiple values of N_c and the minimized WSS is calculated for each so as to determine the smallest N_c beyond which the WSS doesn't decrease much with the increase in N_c .

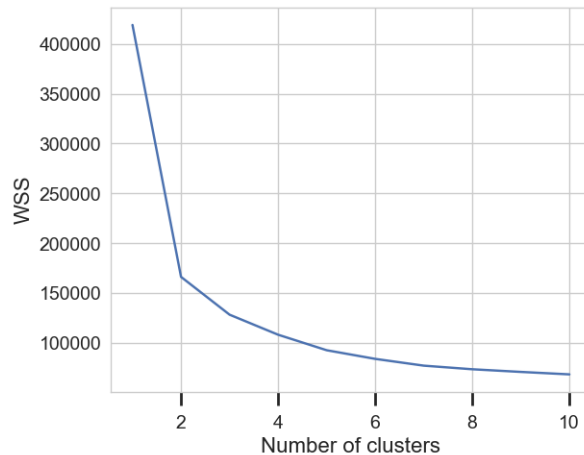


Figure 7: Elbow Plot for the optimal number of clusters

The elbow method suggests that the value of WSS doesn't decrease much after $N_c = 4$. While block bootstrapping considers the temporal correlations between the observed errors, dividing each day's demand vectors into clusters of similar days results in almost constant variance on the model residual errors within the clusters.

4.3. Performance Metrics

The Cluster-based Block Bootstrapping (CBB) method, proposed in the next section makes use of the residual blocks and clustering to output the estimated distribution of the forecast for a given time. Our interest is in finding the quantile values during the time interval i within which the values of electricity demand might lie with a probability $100(1 - \alpha)\%$ which is the size of the confidence interval where $0 \leq \alpha \leq 1$. We will assume a symmetric interval for simplicity where the upper quantile of demand value at $(\alpha/2)$ is defined by $u_{\alpha,i}^j$ and the lower quantile at $(1 - \alpha/2)$ is determined by $l_{\alpha,i}^j$ for the time interval i and day j .

In order to compare different algorithms for interval estimation at confidence level $100(1 - \alpha)\%$ we use the *Winkler Score* ($WS(\alpha)$) and *Coverage Probability* ($CP(\alpha)$) which are defined as follows. Proposed by [Winkler \(1972\)](#), $WS(\alpha)$ is used to evaluate the prediction interval for time series. For observed data y_i^j during the i_{th} time interval, j_{th} day and α confidence level $WS(\alpha)_i^j$ is described by [Hyndman et al. \(2021\)](#) as,

$$WS(\alpha)_i^j = \begin{cases} u_{\alpha,i}^j - l_{\alpha,i}^j + \frac{1}{\alpha}(l_{\alpha,i}^j - y_i^j) & \text{if } y_i^j < l_{\alpha,i}^j, \\ u_{\alpha,i}^j - l_{\alpha,i}^j & \text{if } l_{\alpha,i}^j \leq y_i^j \leq u_{\alpha,i}^j, \\ u_{\alpha,i}^j - l_{\alpha,i}^j + \frac{1}{\alpha}(y_i^j - u_{\alpha,i}^j) & \text{if } y_i^j > u_{\alpha,i}^j. \end{cases}$$

For the j th day, the values of $WS_{\alpha,i}^j$ are averaged over all $i \in I$, and the final WS_{α} for the test set is obtained by averaging over all the day indices $j \in J$ as

$$WS(\alpha) = \frac{1}{|J|} \sum_{j \in J} \sum_{i \in I} \frac{WS_{\alpha,i}^j}{|I|}.$$

The $WS(\alpha)_i^j$ assumes the length of the prediction interval when the observed value of electricity demand y_i^j during time i falls with the prediction interval. If the observed value falls outside then the penalty is proportional to the length denoting how far y_i^j is outside the prediction interval. The WS score for the one-day time series is the average of $CP(\alpha)$ explained in [Hyndman et al. \(2002\)](#) is a measure of the proportion of times the observed values of electricity demand y_i^j lie inside the prediction interval $[l_{\alpha,i}^j, u_{\alpha,i}^j]$ and is defined as,

$$CP(\alpha) = \frac{1}{|J|} \sum_{j \in J} \sum_{i \in I} \frac{\mathbb{1}_{[l_{\alpha,i}^j \leq y_i^j \leq u_{\alpha,i}^j]}}{|I|}$$

$$\begin{aligned} \text{where, } \mathbb{1}_{[l_{\alpha,i}^j \leq y_i^j \leq u_{\alpha,i}^j]} &= 1 \quad \text{when } [l_{\alpha,i}^j \leq y_i^j \leq u_{\alpha,i}^j] \\ &= 0 \quad \text{otherwise.} \end{aligned}$$

A wide prediction interval would lead to high CP values leading to conservative prediction, WS values would penalize the wide intervals. Thus a balance is to be maintained between both scores to get better prediction results.

5. Cluster Block Bootstrap Algorithm (CBB)

In the previous section, we saw the methods to bootstrap residual blocks and to create clusters of similar days. In this section, we will combine these

two methods together to generate the prediction intervals for one-day ahead forecasts. In the first step, we shall form the clusters of the index of similar days using the k-means clustering algorithm on the demand pattern y^j for $j \in J$. As defined in Section 4.2, the number of clusters denoted by N_c has to be initialized for the k-means clustering algorithm to work, and through the elbow method, the total number of clusters, N_c is set at 4. The label of each cluster represented by C_k has a centroid at \bar{y}_{C_k} where $k \in 1, \dots, 4$. We represent the index of days clustered together in the k_{th} cluster as $\{(1), \dots, (|C_k|)\}$, where $|C_k|$ denotes the size of the k_{th} cluster and $\{(1), \dots, (|C_k|)\}$ are the clustered training data days partitioned off training set labeled I such that $\{(1), \dots, (|C_k|)\} \in I$.

The next step is to train the ML model \hat{f} using the training data (\mathbf{X}_i^j, y_i^j) and get the residual errors z_i^j on the training set j . These training errors are stored in the memory set E defined in Equation (2). The memory set of residuals E is then partitioned to form the cluster memory set M_k , where M_k is selected according to the days indexed in cluster C_k . Thus for every cluster label $C_k \in \{(1), \dots, (|C_k|)\}$ we get $M_k = \{z^{(1)}, \dots, z^{(|C_k|)}\}$. Using Equation (4) the set M_k can be denoted in terms of residual blocks

$$M_k = \{(B_1^{(1)}, \dots, B_b^{(1)}), (B_1^{(2)}, \dots, B_b^{(2)}), \dots, (B_1^{(|C_k|)}, \dots, B_b^{(|C_k|)})\}$$

where number of blocks, $b = 16$, and length of residual vector $n = 96$ such that $n = b \times l$ as defined in Section 4.1.

The model \hat{f} , the clustered residual sets M_k and the centroid of the clusters \bar{y}_{C_k} for $k \in (1, \dots, N_c)$ are now ready to evaluate the point estimates and construct the prediction intervals. The ML model \hat{f} , is used to get the point estimates $\hat{y}^{j'}$ for test day j' for $j' \in J'$, i.e., the first quarter of the year 2022. The closeness of $y^{j'}$ which is a vector of size 96, is evaluated with every cluster's centroid using the distance metric $d(y^{j'}, \bar{y}_{C_k})$ and the closest k_{th} residual cluster memory M_k is selected to bootstrap the block residuals for the j'_{th} test day.

The test day is also divided into 16 non-overlapping blocks of size 6, and for the i_{th} interval block of the test day, we bootstrap $N = 1000$ times, residual blocks $B_i^{(n)}$ from the selected cluster M_k randomizing on n such that $n \in (1, \dots, |C_k|)$ and repeat this process for each $i \in (1, \dots, 16)$. Then for the i_{th} time interval block we can get N bootstrap residual block samples and

build $\mathbf{B}_i = (B_1^*, \dots, B_N^*)_i$ ¹. The sets $\mathbf{B}_1, \dots, \mathbf{B}_{16}$ are then joined sequentially to form the prediction interval for the test day.

Due to the over-fitting issues seen in Section 3.2, the residuals bootstrapped from the training set alone results in narrow prediction intervals. The memory of the clustering algorithm can be made adaptive in a way where the training errors are replaced by the errors of the ML model on the test set. Thus we don't use the static cluster residual set M_k from the training data but we keep updating it with the newest residual errors on the observed day in the test data and use the updated M_k to bootstrap for the next day. The update scheme for an observed day j' linked to the cluster is done by selecting the j_{th} day in the training set such that $j' = j$. Then replace and update $z^j = z^{j'}$ in the cluster and recalculate the clusters and their centroids in the interval with a specific update frequency.

6. Results

In this section, we will compare the results of the CBB algorithm for constructing the prediction intervals with other bootstrapping methods like the bootstrap aggregating algorithm and block bootstrap without clustering. The experiments are carried out using the ML models for point estimation mentioned in Section 3. The performance of various combinations of bootstrap methods and ML models is discussed as follows. For ease of notation, we will use WS and CP instead of $WS(\alpha)$ and $CP(\alpha)$ respectively in the following sections.

6.1. Bootstrap Aggregating

The performance of the CBB algorithm is compared against the bootstrap aggregating algorithm, also called bagging. For bootstrap aggregating, multiple replicates or simulated copies of the training data (\mathbf{X}_i^j, y_i^j) are made and an ML model is fitted to each. The first step of this process is to fit the ML model on the original training data and then obtain the residual set E without clusters following a similar procedure to CBB. Then the blocks of residuals are bootstrapped from the training memory E and the original observed demand y_i^j is perturbed to make new copies of y_i^{j*} . Thus, a simulated version of the training set $(\mathbf{X}_i^j, y_i^{j*})$ is obtained. This process is replicated

¹The star notation on x^* indicates that x^* isn't the real data set but the randomized, re-sampled or bootstrapped version of x

N times and the ML model is trained on these N simulated training sets. For every trained model, a trajectory of future electricity demand forecast is obtained on the test set and thus N trajectories are obtained. In this paper, we use $N = 1000$ and the details of the performance of this algorithm for LR, GBR, and LGBM ML models are discussed further.

ML Model	Metrics	$(1-\alpha)100\%$				Training time (sec)
		85	90	95	99	
LR	<i>WS</i>	7.52	8.608	10.266	13.394	498.715
	<i>CP</i>	0.785	0.848	0.917	0.974	
GBR	<i>WS</i>	7.549	8.431	9.711	12.018	529.148
	<i>CP</i>	0.791	0.848	0.905	0.96	
LGBM	<i>WS</i>	7.811	8.921	10.64	13.739	1092.882
	<i>CP</i>	0.815	0.887	0.951	0.986	

Table 2: Model performance for Bootstrap Aggregating

Table 2 represents performance of bootstrap aggregate model on the test data. *WS* for the GBR model is the lowest compared to LR and LGBM which shows that the intervals for GBR are narrower. Ideally, the value of *CP* should be as close as possible to the interval size $100(1 - \alpha)\%$. The best *CP* values are attained by the LGBM model as the values are much closer to the size of the confidence intervals. A good model would be one for which the value of *WS* is lower simultaneously with higher *CP* values. A high *WS* with a relatively higher *CP* value is caused due to conservative estimates of upper and lower confidence levels. On the other hand, lower *WS* values with low *CP* scores suggest a higher magnitude of violations of observed data beyond the confidence limits. Another important point to note is the computation time required for the interval prediction. Bootstrap aggregating models are computationally expensive due to model training on multiple simulated training sets. A new synthetic training set is simulated and an ML model is trained on this set to generate a new trajectory of forecasted values of electricity demand.

6.2. Block Bootstrap

The results of the Block Bootstrap algorithm without clustering are discussed in this section. We will simply refer to it as the Block Bootstrap algorithm. The prediction intervals are constructed similarly to CBB algorithm, i.e., by bootstrapping the non-overlapping residuals block but without

clustering the similar days. This will help us understand the effect of clustering done by the CBB algorithm by only using the block bootstrapping scheme.

ML Model	Metrics	$(1-\alpha)100\%$				Training time (sec)
		85	90	95	99	
LR	<i>WS</i>	8.529	9.531	11.229	16.007	15.73
	<i>CP</i>	0.741	0.807	0.885	0.959	
GBR	<i>WS</i>	7.973	8.735	10.005	12.453	34.95
	<i>CP</i>	0.804	0.861	0.922	0.981	
LGBM	<i>WS</i>	7.887	8.754	10.113	13.2	23.42
	<i>CP</i>	0.741	0.806	0.888	0.969	

Table 3: Model performance for Block Bootstrap

The performance of Block Bootstrap is shown in Table 3. We see that the GBR model achieves better performance on both the *WS* and *CP* values compared to the LR and LGBM models (except for *WS* value for 85% confidence interval size). The GBR Block Bootstrap models also have better *CP* values compared to the GBR Bootstrap Aggregate algorithm with a significant reduction in computation time.

6.3. CBB algorithm

The performance of the CBB algorithm proposed in Section 5 is shown in Table 4. The *WS* values for the LGBM model are consistently lower as compared to the LR and GBR models but the *CP* values are not high enough. The best *CP* values are attained by the GBR model followed by LR with only a slight trade-off on the *WS* values compared to LGBM. The CBB algorithm gains computation time over the block bootstrap method due to the clustering process but outputs a better prediction interval. The computation time when compared to the bootstrap aggregating method is still considerably lower. Figure 8 shows the one-day moving average of the demand prediction at 90% confidence interval and observed demand for the test set.

Until now we have just compared the performance of the ML models within each of the bootstrap algorithms. We will now compare the performance across all the bootstrapping algorithms based on the *WS* and *CP* scores they achieve with the ML models, which will help us to analyze the effect of clustering.

ML Model	Metrics	$(1-\alpha)100\%$				Training time (sec)
		85	90	95	99	
LR	<i>WS</i>	8.259	9.127	10.518	14.92	106.231
	<i>CP</i>	0.81	0.864	0.928	0.972	
GBR	<i>WS</i>	8.387	9.266	10.73	12.657	143.75
	<i>CP</i>	0.839	0.89	0.949	0.987	
LGBM	<i>WS</i>	8.059	8.93	10.345	12.5	112.626
	<i>CP</i>	0.777	0.838	0.91	0.983	

Table 4: Model performance for CBB algorithm

6.4. Comparative analysis

The comparison of the bootstrapping algorithms with different combinations of the ML models according to the confidence interval sizes is shown in Figure 9. For each confidence interval size $(1 - \alpha)100\%$, the values of $CP(\alpha)$ are plotted against $WS(\alpha)$.

In the plot for 85% CI, the rightmost point represents the highest CP value attained by CBB built on the GBR model. The block bootstrap model based on LR has the second-best CP value but a better WS than the CBB GBR model. Identical results are seen in the 90% interval, but the LR block bootstrap model almost achieves the CP of CBB GBR algorithm with a smaller WS . However, the LR block bootstrap model slightly outperforms the GBR CBB algorithm for 95% CI. The GBR CBB algorithm has the best CP for the 99% interval with a lower WS value. The higher CP values for the CBB algorithm based on GBR show the effect of bootstrapping from clusters of similar days.

LGBM with bootstrap aggregating has the lowest CP and highest WS values for all the confidence intervals indicating higher penalties due to the narrow prediction interval size. The analysis suggests that the CBB algorithm achieves higher coverage than the other algorithms especially when GBR is used as a point estimate ML model.

7. Conclusion

The proposed CBB algorithm uses point forecasts of the ML model to build prediction intervals based on residuals of the ML model. The interval prediction CBB algorithm based on the ML point estimates has better CP

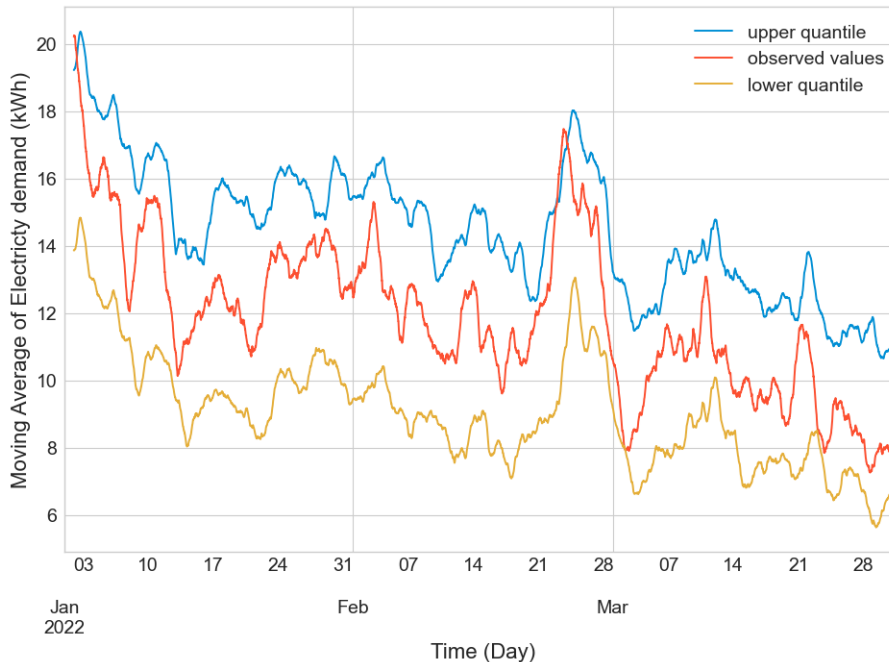


Figure 8: Moving Average of 90% Prediction interval on test data

compared to bootstrap aggregating and block bootstrap methods with a relatively lower WS value, especially for GBR. The CBB algorithm uses the concept of similar days according to which the pattern of electricity demand doesn't deviate much from historical usage and errors of the ML model for similar days would be similar. These residual errors then can be clustered together and the prediction interval of the test day is built by bootstrapping residuals from the cluster closest to point forecast of the test day according to some distance metric. Introducing clustering of similar days leads to better CP for every confidence interval with comparable WS when compared to just block bootstrap without clustering. The CBB algorithm builds upon the lesser time taken by the just block bootstrapping and competes with the bootstrap aggregation.

In comparison, the error metrics of the CBB algorithm are better than bootstrap aggregating algorithm, beating it on the CP scores when GBR is used as an ML model. The major highlight is reduction in computation time required by the CBB algorithm when compared to bootstrap aggregating. The experiment is carried out on residential sites of the EULR data in

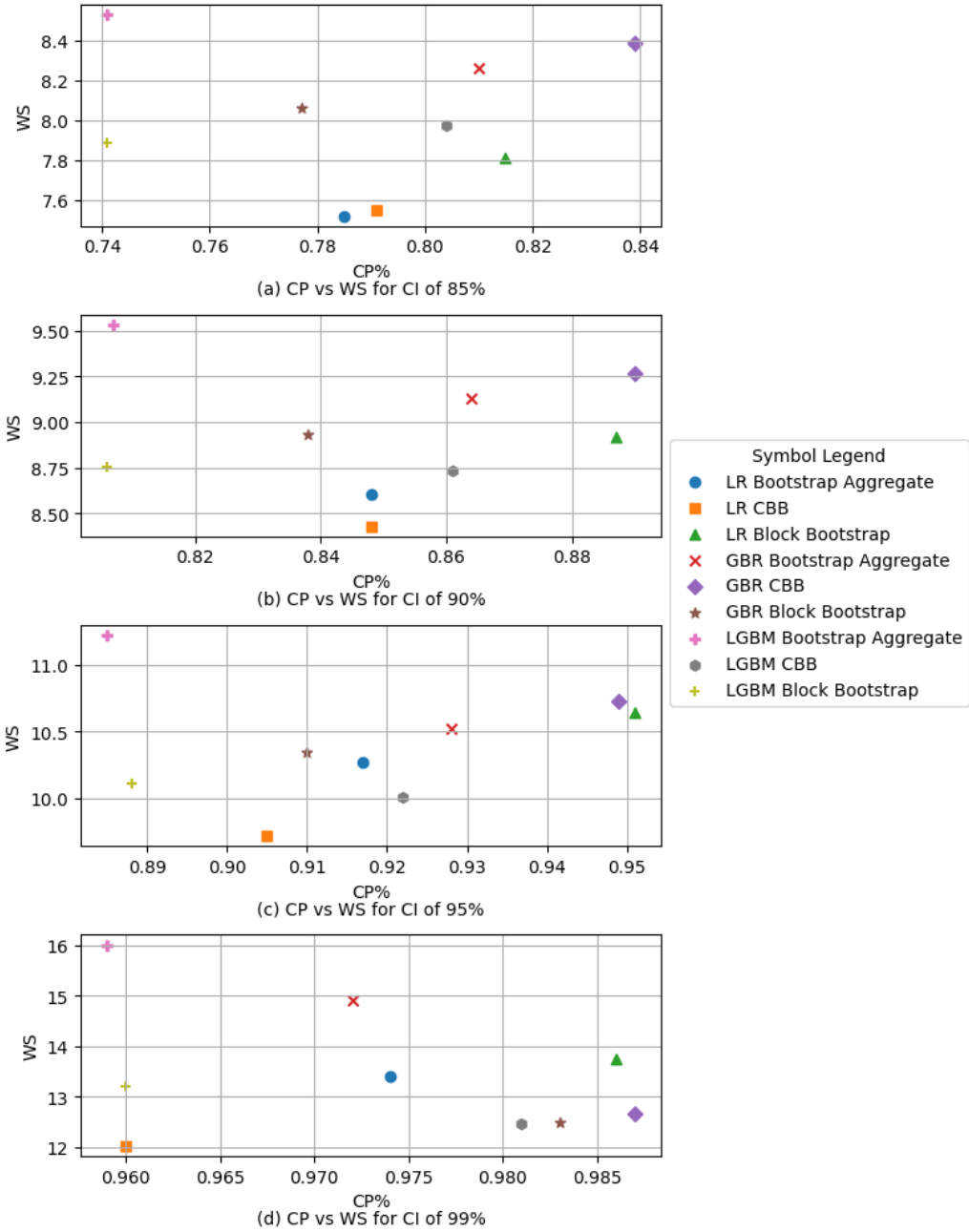


Figure 9: CP vs WS plots of (a) 85% , (b) 90% ,(c) 95% and (d) 99% confidence intervals for combinations of ML models and interval estimation algorithm

Washington state and shows the effectiveness of using bootstrapping methods to generate prediction intervals.

8. Future Work

In this work, we have used a k-means clustering algorithm to group together similar days of electricity demand. The residual estimates to construct the interval for the prediction day are bootstrapped from the closest cluster to the point estimates of the prediction day. While we see that this method leads to better coverage probabilities for most of the confidence levels, additional features could be used to generate the clusters on the basis of exogenous variables. Clustering algorithms like density-based clustering or fuzzy clustering could capture more complex patterns in the data. Furthermore, the method of measuring the distance from clusters' centroids before prediction could lead to anomaly detection. The main aspect of using tree-based ensemble models in this research was the success of these models in time-series forecasting. Similarly, recent work on temporal fusion transformers by [Lim et al. \(2021\)](#) has been proven to work on a variety of real-world datasets and could be used to obtain better point estimates on multi-horizon forecasting.

Acknowledgements

The authors gratefully acknowledge funding from Triad National Security LLC under the grant from the Department of Energy National Nuclear Security Administration (award no. 89233218CNA000001), titled "An Integrated Approach for Managing Microgrids with Uncertain Renewable Sources, Demand Response, and Energy Markets".

References

- Ahmad, A.S., Hassan, M.Y., Abdullah, M.P., Rahman, H.A., Hussin, F., Abdullah, H., Saidur, R., 2014. A review on applications of ANN and SVM for building electrical energy consumption forecasting. *Renewable and Sustainable Energy Reviews* 33, 102–109. doi:[10.1016/J.RSER.2014.01.069](https://doi.org/10.1016/J.RSER.2014.01.069).
- Bergmeir, C., Hyndman, R.J., Benítez, J.M., 2016. Bagging exponential smoothing methods using STL decomposition and BoxCox transformation. *International Journal of Forecasting* 32, 303–312. doi:[10.1016/J.IJFORECAST.2015.07.002](https://doi.org/10.1016/J.IJFORECAST.2015.07.002).
- Bojer, C.S., Meldgaard, J.P., 2021. Kaggle forecasting competitions: An overlooked learning opportunity. *International Journal of Forecasting* 37, 587–603. doi:[10.1016/J.IJFORECAST.2020.07.007](https://doi.org/10.1016/J.IJFORECAST.2020.07.007).
- Clements, A.E., Hurn, A.S., Li, Z., 2016. Forecasting day-ahead electricity load using a multiple equation time series approach. *European Journal of Operational Research* 251, 522–530. doi:[10.1016/J.EJOR.2015.12.030](https://doi.org/10.1016/J.EJOR.2015.12.030).
- Clements, M.P., Kim, J.H., 2007. Bootstrap prediction intervals for autoregressive time series. *Computational Statistics & Data Analysis* 51, 3580–3594. doi:[10.1016/J.CSDA.2006.09.012](https://doi.org/10.1016/J.CSDA.2006.09.012).
- Cleveland, R., Cleveland, W., McRae, J.E., Terpenning, I.J., 1990. STL: A seasonal-trend decomposition procedure based on loess (with discussion). *Journal of Official Statistics* URL: <https://api.semanticscholar.org/CorpusID:64570714>.
- Efron, B., 1979. Bootstrap Methods: Another Look at the Jackknife. *The Annals of Statistics* 7, 1 – 26. doi:[10.1214/aos/1176344552](https://doi.org/10.1214/aos/1176344552).
- Elsaraiti, M., Ali, G., Musbah, H., Merabet, A., Little, T.A., 2021. Time series analysis of electricity consumption forecasting using arima model. 2021 IEEE Green Technologies Conference (GreenTech) , 259–262doi:[10.1109/GreenTech48523.2021.00049](https://doi.org/10.1109/GreenTech48523.2021.00049).
- Espinoza, M., Joye, C., Belmans, R., De Moor, B., 2005. Short-term load forecasting, profile identification, and customer segmentation: a methodology based on periodic time series. *IEEE Transactions on Power Systems* 20, 1622–1630. doi:[10.1109/TPWRS.2005.852123](https://doi.org/10.1109/TPWRS.2005.852123).

- Fildes, R., Randall, A., Stubbs, P., 1997. One Day Ahead Demand Forecasting in the Utility Industries: Two Case Studies. *The Journal of the Operational Research Society* 48, 15. doi:[10.2307/3009939](https://doi.org/10.2307/3009939).
- Hartigan, J.A., Wong, M.A., 1979. Algorithm AS 136: A K-Means Clustering Algorithm. *Applied Statistics* 28, 100. doi:[10.2307/2346830](https://doi.org/10.2307/2346830).
- Harvey, A., Statistical, S.K.J.o.t.A., 1993, u., 1993. Forecasting hourly electricity demand using time-varying splines. *Taylor & Francis* 88, 1228–1236. doi:[10.1080/01621459.1993.10476402](https://doi.org/10.1080/01621459.1993.10476402).
- Hippert, H., Pedreira, C., Souza, R., 2001. Neural networks for short-term load forecasting: a review and evaluation. *IEEE Transactions on Power Systems* 16, 44–55. doi:[10.1109/59.910780](https://doi.org/10.1109/59.910780).
- Hong, T., Fan, S., 2016. Probabilistic electric load forecasting: A tutorial review. *International Journal of Forecasting* 32, 914–938. doi:[10.1016/j.ijforecast.2015.11.011](https://doi.org/10.1016/j.ijforecast.2015.11.011).
- Hyndman, R.J., Athanasopoulos, G., 2021. *Forecasting: Principles and Practice*. 3 ed., OTexts: Melbourne, Australia. URL: <https://otexts.com/fpp3/>. accessed on 4 July 2023.
- Hyndman, R.J., Koehler, A.B., Snyder, R.D., Grose, S., 2002. A state space framework for automatic forecasting using exponential smoothing methods. *International Journal of Forecasting* 18, 439–454. doi:[10.1016/S0169-2070\(01\)00110-8](https://doi.org/10.1016/S0169-2070(01)00110-8).
- Hrdle, W., Horowitz, J., Kreiss, J.P., 2003. Bootstrap methods for time series. *International Statistical Review* 71, 435–459. doi:<https://doi.org/10.1111/j.1751-5823.2003.tb00485.x>.
- Kong, W., Dong, Z.Y., Jia, Y., Hill, D.J., Xu, Y., Zhang, Y., 2019. Short-Term Residential Load Forecasting Based on LSTM Recurrent Neural Network. *IEEE Transactions on Smart Grid* 10, 841–851. doi:[10.1109/TSG.2017.2753802](https://doi.org/10.1109/TSG.2017.2753802).
- Lago, J., Marcjasz, G., De Schutter, B., Weron, R., 2021. Forecasting day-ahead electricity prices: A review of state-of-the-art algorithms, best practices and an open-access benchmark. *Applied Energy* 293, 116983. doi:[10.1016/J.APENERGY.2021.116983](https://doi.org/10.1016/J.APENERGY.2021.116983).

- Lee, C., Liu, C., Mehrotra, S., Bie, Z., 2015. Robust distribution network reconfiguration. *IEEE Transactions on Smart Grid* 6, 836–842. doi:[10.1109/TSG.2014.2375160](https://doi.org/10.1109/TSG.2014.2375160).
- Li, Z., Hurn, A.S., Clements, A.E., 2017. Forecasting quantiles of day-ahead electricity load. *Energy Economics* 67, 60–71. doi:[10.1016/J.ENECO.2017.08.002](https://doi.org/10.1016/J.ENECO.2017.08.002).
- Lim, B., Ark, S., Loeff, N., Pfister, T., 2021. Temporal fusion transformers for interpretable multi-horizon time series forecasting. *International Journal of Forecasting* 37, 1748–1764. doi:<https://doi.org/10.1016/j.ijforecast.2021.03.012>.
- Mignani, S., Rosa, R., 1995. The moving block bootstrap to assess the accuracy of statistical estimates in Ising model simulations. *Computer Physics Communications* 92, 203–213. doi:[10.1016/0010-4655\(95\)00114-7](https://doi.org/10.1016/0010-4655(95)00114-7).
- Mocanu, E., Nguyen, P.H., Gibescu, M., Kling, W.L., 2016. Deep learning for estimating building energy consumption. *Sustainable Energy, Grids and Networks* 6, 91–99. doi:[10.1016/J.SEGAN.2016.02.005](https://doi.org/10.1016/J.SEGAN.2016.02.005).
- Mori, H., Kobayashi, H., 1996. Optimal fuzzy inference for short-term load forecasting. *IEEE Transactions on Power Systems* 11, 390–396. doi:[10.1109/59.486123](https://doi.org/10.1109/59.486123).
- Northwest Energy Efficiency Alliance, 2020. Home Energy Metering Study. URL: <https://neea.org/img/documents/EULR-HEMS-User-Guide.pdf>. accessed on 4 July 2023.
- Pan, L., Politis, D.N., 2016. Bootstrap prediction intervals for linear, non-linear and nonparametric autoregressions. *Journal of Statistical Planning and Inference* 177, 1–27. doi:<https://doi.org/10.1016/j.jspi.2014.10.003>.
- Pecan Street Inc. Dataport, . Dataport Pecan Street Inc. URL: <https://www.pecanstreet.org/dataport/>. accessed on 4 July 2023.
- Politis, D.N., White, H., 2006. Automatic Block-Length Selection for the Dependent Bootstrap. <http://dx.doi.org/10.1081/ETC-120028836> 23, 53–70. doi:[10.1081/ETC-120028836](https://doi.org/10.1081/ETC-120028836).

- Singh, K., 1981. On the Asymptotic Accuracy of Efron's Bootstrap. *The Annals of Statistics* 9, 1187 – 1195. doi:[10.1214/aos/1176345636](https://doi.org/10.1214/aos/1176345636).
- Son, J., Cha, J., Kim, H., Wi, Y.M., 2022. Day-Ahead Short-Term Load Forecasting for Holidays Based on Modification of Similar Days' Load Profiles. *IEEE Access* 10, 17864–17880. doi:[10.1109/ACCESS.2022.3150344](https://doi.org/10.1109/ACCESS.2022.3150344).
- Stine, R.A., 1985. Bootstrap Prediction Intervals for Regression. *Journal of the American Statistical Association* 80, 1026. doi:[10.2307/2288570](https://doi.org/10.2307/2288570).
- U.S. Energy Information Administration, . Hourly electricity consumption varies throughout the day and across seasons. URL: <https://www.eia.gov/todayinenergy/detail.php?id=42915>. accessed on 4 July 2023.
- Winkler, R.L., 1972. A decision-theoretic approach to interval estimation. *Journal of the American Statistical Association* 67, 187–191. doi:[10.1080/01621459.1972.10481224](https://doi.org/10.1080/01621459.1972.10481224).
- Zhang, R., Dong, Z.Y., Xu, Y., Meng, K., Wong, K.P., 2013. Short-term load forecasting of Australian national electricity market by an ensemble model of extreme learning machine. *IET Generation, Transmission and Distribution* 7, 391–397. doi:[10.1049/IET-GTD.2012.0541](https://doi.org/10.1049/IET-GTD.2012.0541).